Facile synthesis of AA'B- and ABC-type polypept(o)ide miktoarm star polymers utilizing polysarcosine end group functionalization for core introduction

Capelôa, L.; Schwiertz, D.; Barz, M.

European Polymer Journal 187 (2023) 111896

Contents lists available at ScienceDirect

European Polymer Journal

journal homepage: www.elsevier.com/locate/europolj

Facile synthesis of AA'B- and ABC-type polypept(o)ide miktoarm star polymers utilizing polysarcosine end group functionalization for core introduction

Leon Capelôa, David Schwiertz, Matthias Barz *

Biotherapeutics Division, Leiden Academic Centre for Drug Research (LACDR), Leiden University, Einsteinweg 55, Leiden 2333CC, The Netherlands
Department of Dermatology, University Medical Center, Johannes Gutenberg-University Mainz (JGU), Obere Zahlbacher Straße 63, 55131 Mainz, Germany

ARTICLE INFO

Keywords:
ROP
NCA
Polysarcosine
PeptoMiktoStars

ABSTRACT

Miktoarm star polymers display asymmetric architectures with combinations of multiple polymeric arms of different chemical nature emanating from a shared core. Their unique structure–property relationships in comparison to linear counterparts (with same molecular weight) make these architectures interesting for the design of novel polymeric species and the development of nanosized delivery systems. However, the synthesis of such structures is often demanding. Based on polypept(o)ides, we herein report on the synthesis of AA'B- and ABC-type miktoarm star polymers by introducing a multifunctional lysine end group to a polysarcosine (pSar) chain end, comprising orthogonal amine-protective groups. Therefore, each polymeric arm could be synthesized separately by living ring-opening polymerization (ROP) of respective *N*-carboxyanhydrides (NCAs), offering high reaction control and a resulting structure completely based on amino acids. We demonstrate the utility and versatility of this approach by designing a small, asymmetric and big AA'B miktoarm star polymer comprising two pSar arms with chain lengths of ~50 or ~150 in different combinations and a poly(N_ε-trifluoroacetate-lysine) (pLys(TFA)) arm, as well as an ABC architecture by introducing a poly(γ-benzyl-glutamate) (pGlu(OBn)). ^{1}H NMR, including ^{1}H DOSY experiments, as well as size-exclusion chromatography (*SEC*) proof the successful and controlled synthesis of asymmetric miktoarm star polymers with precise control over degree of polymerization of the individual arms with narrow molecular weight distributions.

1. Introduction

In 1990, Mays described the first synthesis of a branched polymeric structure comprising arms of different chemical nature sharing a central core, which was two years later defined as "miktorarm" star polymers (from greek μικτός or miktós, engl. mixed) by Iatrou and Hadjichristidis [1,2]. In general, these structures are classified into $A_xB_yC_z$ categories, where A, B, C description displays differences from slight variations in molecular weights to comprising totally different chemical nature of the polymeric arms and x,y,z depict their quantity per star polymer [3–6]. Especially in the field of synthetic polymer chemistry miktoarm architectures have raised interest due to the broad variety of chemical functionalities and design possibilities. But also in the field of nanomedicine these structures provide the desirable ability to tailor carrier properties by arm length, composition, ratios, quantity or chemical nature [5,7–9]. Commonly the synthesis of miktoarm star polymers is performed either by the classical arm-first and core-first synthetic approaches, where either pre-polymerized arms are linked to a core or a multifunctional core is used for polymerization of different arms respectively. Also solid-phase synthetic strategies have been applied for star-shaped polymers [10]. For biological approaches crossover techniques of core- and arm-first method are more frequently applied, probably based on the ease and variety of commercial available heterotelechelic polyethylene glycols (PEGs), the gold-standard as hydrophilic shielding material of drug carriers. These PEGs are simple to modify and can be used as multi-macroinitiator or coupled to a junction of previous polymerized multi-block structures to create miktoarm architectures [11–13]. While e.g., serinol- or lysine-functionalized PEGs are common macroinitators for AB_2 miktoarm stars [14–17], only a few examples can be found, where the introduced functional end group of a polymer was utilized to perform multiple and independent polymerizations to generate individual arms [18–20].

* Corresponding author.
E-mail address: m.barz@lacdr.leidenuniv.nl (M. Barz).

https://doi.org/10.1016/j.eurpolymj.2023.111896
Received 9 January 2023; Received in revised form 31 January 2023; Accepted 7 February 2023
Available online 10 February 2023

However, despite the broad use of PEG, emerging evidences reveal the necessity for an alternative shielding material in nanosized delivery systems [21] to circumvent drawbacks including the accelerated blood clearance (ABC) phenomenon caused by interaction with antiPEG-antibodies [22,23], complement activation [24] or elevated cytokine excretion as acute immune response [25]. In recent years, the polypeptoid pSar has evolved as a most promising PEG-alternative by possessing comparable solution properties [26], improved immunogenicity [27], protein resistance [28], and therefore enabling the synthesis of carrier systems with neglectable protein corona [29,30]. Therapeutic efficiency could recently been presented for pSar-based lipid formulations [25,31], polyplexes,[32,33] polymeric micelles,[32,34,35] star polymers [36–39] and molecular polymer brushes [40,41]. All these systems combine pSar with polypeptide segments and therefore belong to the Polypept(o)ides [42,43]. Synthetic access to polypept(o)ides is provided by sequential ROP of respective NCAs, enabling precise control over chain length and size distribution under optimized reaction conditions, which offers a broad range of polymer microstructures [44–47]. In terms of star polymers mainly symmetric star architectures are described based on polypept(o)ides ranging from 3- to 8-arm structures based on small molecule core-initiators [36–38,48,49] up to 32-arm architectures based on lysine-dendrimer initiators [50]. The first and only miktoarm star polymers on polypept(o)ides, so-called PeptoMiktoStars, were described by Schwiertz *et al.*, presenting A_3B and AB_3 architectures composed of pSar and pGlu(OBn) arms [51]. All mentioned star polymers have been synthesized by the core-first method.

Combining the previously described modern methodology of crossover star synthesis with polypept(o)idic material, we herein report on the facile synthesis of AA'B- and ABC-type miktoarm stars by introducing a multifunctional lysine end group at a pSar polymer chain with orthogonal protective groups, enabling controlled and separate synthesis of each arm by amine-initiated ROP of respective NCAs upon selective amine deprotection. Thus, this method enables control over chemical nature (in terms of polypept(o)ides), chain length and end group functionality of each single arm and generates a polymeric star architecture that relies 100 % on amino acid repeating units (including the core). Therefore, we are able to present novel polymeric species, close the gap between linear and A_3B architectures and introduce a novel synthetic route to generally access PeptoMiktoStars.

2. Experimentals

Materials, solvents and chemicals were principally purchased from Sigma Aldrich and used as received unless stated otherwise. *N,N*-Dimethylformamide (99.8 %, extra dry, over molecular sieve) was bought from ACROS ORGANICS and handled under exclusion of light and oxygen. Prior to use as solvent for polymerization reactions, it was purified by multiple freeze–pumpthaw cycles to remove residual amine impurities. Neopentylamine was purified/dried by stirring over potassium hydroxide for three days, subsequential distillation into a pre-dried Schlenk tube equipped with molecular sieve and stored at −20 °C under light and oxygen exclusion. Trifluoracetic acid was purchased from Carl Roth. To monitor NCA polymerization progress attenuated total reflectance Fourier transformed infrared (ATR-FTIR) spectroscopy was utilized, correlating progress to respective NCA carbonyl bands at 1853 cm^{-1} and 1786 cm^{-1}. Measurements were performed at ambient temperature on a FT/IR-4100 (JASCO) equipped with an ATR sampling accessory (MIRacle TM, Pike Technologies) and spectra were visualized as well as analyzed using Spectra Manager 2.0 software (JASCO). Polymer analytics have been performed by ^{1}H NMR spectroscopy, including Diffusion Ordered Spectroscopy (DOSY) experiments, carried out on a Bruker Avance I (AV-500 MHz) at ambient temperature and a concentration of 15 mg/mL. MestReNova software (version 12.0.2) was used to analyze spectra with calibration by the solvent signal [52]. Deuterated *N,N*-Dimethyl sulfoxide as solvent for NMR experiments was purchased from Deutero GmbH. Further, polymers have been analyzed by size exclusion chromatography (*SEC*), in detail Gel permeation chromatography (GPC) utilizing hexafluoroisopropanol as eluent containing 3 g/L potassium trifluoroacetate. Both chemicals were bought from Fluorochem. Measurements were carried out at 40 °C with a flow rate of 1 mg/mL and calibrated by the toluene signals as internal standard. The column setup (PFG columns with modified silica gel, particle size 7 μm, porosity: 100 Å + 1000 Å) as well as the PSS WinGPC software to monitor and analyze elution diagrams were purchased from PSS Polymer Standard Service GmbH. Millipore water was obtained from a Milli-Q A + system with resistivity of 18.2 MΩ/cm and values for organic carbon of <5 ppb. Lyophilization to isolate polymers from aqueous solutions was performed on a VirTis BenchTop Pro Freeze Dryer from SP Scientific Products.

2.1. Polymer synthesis

Polymeric structures derived from amine-initiated ROP of NCAs. Respective NCA monomers from sarcosine (Sar), N_ε-trifluoroacetyl-L-lysine (Lys(TFA)) and γ-benzyl-L-glutamate (Glu(OBn)) were synthesized and characterized as published previously [43,53]. Polymerization reactions were performed in purified DMF under Schlenk conditions, light exclusion, at 0 °C and final concentrations of around 100 mg/mL.

2.2. Multifunctional Macroinitiator: (Neo)pSar$_{56}$-Lys(Boc)-H

Within a pre-dried Schlenk tube, Sar-NCA (735 mg, 6.39 mmol, 50 eq) was dissolved in 6.5 mL of purified DMF and cooled down to 0 °C. 29.9 μL of neopentylamine (22.3 mg, 0.26 mmol, 2 eq) were dissolved in 1 mL purified DMF. Subsequently, 0.5 mL of the initiator stock solution were added to the NCA. The mixture was stirred under Schlenk conditions and light exclusion until complete monomer conversion, which could be verified by IR after 24 h. After short evacuation of the Schlenk tube, N_α-Fmoc-N_ε-Boc-L-lysine pentafluorophenyl ester (Fmoc-Lys(Boc)-OPfp) (810 mg, 1.28 mmol, 10 eq) was added and the mixture was stirred for 24 h. To increase probability for complete end group functionalization, 42 mg 4-(4,6-Dimethoxy-1,3,5-triazin-2-yl)-4-methylmorpholiniumtetrafluoroborate (DMTMM·BF_4) (0.13 mmol, 1 eq) were added and the mixture stirred for another 24 h. To separate the polymer from DMF, residual capping agents and adjuvants, the solution was added dropwise into an excess of THF for precipitation, subsequently centrifuged (10 min, 4500 rpm, 0 °C) and the supernatant was discarded. The solid was resuspended in fresh solvent and the procedure was repeated twice with THF, then again three times with diethyl ether and finally dried under vacuum to yield 519 mg (yield: 94 %) of a colorless powder. ^{1}H NMR (500 MHz, DMSO-d_6) δ[ppm] = 7.88 (d, $2H_{Fmoc}$, C$H^{4/5}$), 7.73 (t, $2H_{Fmoc}$, C$H^{1/8}$), 7.51 (m, $1H_{Lys}$, N_aH), 7.41 (t, $2H_{Fmoc}$, C$H^{3/6}$), 7.32 (t, $2H_{Fmoc}$, C$H^{2/7}$), 6.77 (m, $1H_{Lys}$, N_eH), 4.38–3.93 (m, $2nH_{Sar}$, CH_2) and ($1H_{Lys}$, $C_\alpha H$) and ($2H_{Fmoc}$, CH_2) and ($1H_{Fmoc}$, CH^9), 3.00–2.73 (m, $3nH_{Sar}$, CH_3) and ($2H_{Lys}$, N_εH-CH_2), 1.63–1.23 ($6H_{Lys}$, C_αH-CH_2-CH_2-CH_2), 1.36 (s, $9H_{Boc}$, C(CH_3)$_3$), 0.86–0.82 (d, $9H_{Neo}$, C(CH_3)$_3$).

To remove the Fmoc-group from the functional Lys end group, the polymer was dissolved in 4 mL of DMF and 1 mL of piperidine (20 % v/v) was added. The mixture was stirred for 6 h. To remove formed dibenzofulvene-piperidine side-product, the mixture was extracted with 5 mL of *n*-hexane four times. For precipitation of the polymeric species, the solution was added dropwise into an excess of THF, followed by centrifugation and discarding of the supernatant. The procedure was repeated by resuspending the polymer two times in THF and another three times in diethyl ether. To ensure complete separation from piperidine, the polymer was diluted in water and dialyzed (MWCO 1 kDa) against 1 L of water for two days, followed by lyophilization to yield a colorless fluffy solid (230 mg, yield: 48 %). ^{1}H NMR (500 MHz, DMSO-d_6) δ [ppm] = 6.77 (m, $1H_{Lys}$, $N_\varepsilon H$), 4.38–3.93 (m, $2nH_{Sar}$, CH_2) and ($1H_{Lys}$, C_aH), 3.00–2.73 (m, $3nH_{Sar}$, CH_3) and ($2H_{Lys}$, N_eH-CH_2),

1.63–1.23 (6H_{Lys}, C_aH-CH_2-CH_2-CH_2), 1.36 (s, 9H_{Boc}, C(CH_3)$_3$), 0.86–0.82 (d, 9H_{Neo}, C(CH_3)$_3$).

For larger macroinitiators, as basis for asymmetric and big stars, equivalents of Sar-NCA have been adjusted to 150 and final dialysis was performed with MWCO 3 kDa.

2.3. AA' Macroinitiator: (Neo)pSar$_{56}$-Lys-pSar$_{53}$(Ac)

Previously synthesized (Neo)pSar$_{56}$-Lys(Boc)-H was used as macroinitiator for polymerization and production of the second arm. 107 mg (Neo)pSar$_{56}$-Lys(Boc)-H (0.025 mmol, 1 eq) were weight into a pre-dried Schlenk tube and dried under vacuum overnight, then dissolved in 1 mL of purified DMF and cooled down to 0 °C. 141 mg Sar-NCA (1.225 mmol, 50 eq) were also dissolved in 1.5 mL of purified DMF and cooled down to 0 °C within a pre-dried Schlenk tube. The solutions were combined and stirred under Schlenk conditions and light exclusion at 0 °C. After 24 h complete monomer consumption was confirmed by IR. Acetylation was performed to inactivate the reactive chain end. Therefore, 83 μL DIPEA (0.49 mmol, 20 eq) were added and the mixture was stirred for 10 min. Subsequently, 23 μL acetic anhydride (0.25 mmol, 10 eq) were added and the mixture was stirred overnight. The solution was added dropwise into an excess of diethyl ether, followed by centrifugation and discarding of the supernatant. The procedure was repeated by resuspending the polymer another two times in diethyl ether. The colorless powder was dried overnight under vacuum (192 mg, yield: 97 %). ^{1}H NMR (500 MHz, DMSO-d_6) δ [ppm] = 6.75 (m, 1H_{Lys}, N$_\varepsilon$H), 4.40–3.86 (m, 2nH_{Sar} and 2mH_{Sar}, CH_2) and (1H_{Lys}, C$_\alpha$H), 2.96–2.69 (m, 3nH_{Sar} and 3mH_{Sar}, CH_3) and (2H_{Lys}, N$_\varepsilon$H-CH_2), 2.00 (d, 3H_{Ac}, CH_3), 1.70–1.22 (6H_{Lys}, C$_\alpha$H-CH_2-CH_2-CH_2), 1.36 (s, 9H_{Boc}, C(CH_3)$_3$), 0.86–0.82 (d, 9H_{Neo}, C(CH_3)$_3$).

To remove the Boc-protective group from the functional Lys core, the polymer was dissolved in 4 mL of water and cooled with an ice bath while stirring. 4 mL of TFA (50 % v/v) were added dropwise, the mixture was stirred for 2 h and another 2 h at ambient temperature. To isolate the polymeric species, the mixture was transferred to a dialysis bag (MWCO 3 kDa) and dialyzed against 1 L of water for three days, followed by lyophilization to yield a colorless fluffy solid (113 mg, yield: 60 %). ^{1}H NMR (500 MHz, DMSO-d_6) δ [ppm] = 6.75 (m, 1H_{Lys}, N$_\varepsilon$H), 4.40–3.86 (m, 2nH_{Sar} and 2mH_{Sar}, CH_2) and (1H_{Lys}, C$_a$H), 2.96–2.69 (m, 3nH_{Sar} and 3mH_{Sar}, CH_3) and (2H_{Lys}, N$_\varepsilon$H-CH_2), 2.00 (d, 3H_{Ac}, CH_3), 1.70–1.22 (6H_{Lys}, C$_\alpha$H-CH_2-CH_2-CH_2), 0.86–0.82 (d, 9H_{Neo}, C(CH_3)$_3$).

For larger A' pSar arms, as basis for asymmetric and big stars, equivalents of Sar-NCA have been adjusted to 150.

2.4. AA'B miktoarm star Polymers: (Neo)pSar$_{56}$-Lys(pLys(TFA)$_{19}$)-pSar$_{53}$(Ac)

Previously synthesized (Neo)pSar$_{56}$-Lys-pSar$_{53}$(Ac) was used as macroinitiator for polymerization and production of the third arm. 100 mg of (Neo)pSar$_{56}$-Lys-pSar$_{53}$(Ac) (0.013 mmol, 1 eq) were weight into a pre-dried Schlenk tube and dried under vacuum overnight, then dissolved in 1 mL of purified DMF and cooled to 0 °C. 70 mg Lys(TFA)-NCA (0.313 mmol, 25 eq) were also dissolved in 1 mL of purified DMF and cooled down to 0 °C within a pre-dried Schlenk tube. The solutions were combined and stirred under Schlenk conditions and light exclusion at 0 °C. After three days complete monomer conversion was confirmed by IR and the polymer isolated by precipitation into diethyl ether, followed by centrifugation and discarding the supernatant. The procedure was repeated twice by resuspending the solid in diethyl ether. Finally, the solid was dried overnight under vacuum to yield 154 mg (yield 77 %) of a colorless solid. ^{1}H NMR (500 MHz, DMSO-d_6) δ [ppm] = 9.39–9-25 (m, 1lH_{Lys}, N$_\varepsilon$H), 8.41–7.67 (br, 1lH_{Lys}, N$_\alpha$H), 4.39–3.81 (m, 2nH_{Sar} and 2mH_{Sar}, CH_2) and (1lH_{Lys}, C$_\alpha$H), 3.16–3.11 (br, 2lH_{Lys}, N$_\varepsilon$H-CH_2), 2.96–2.72 (m, 3nH_{Sar} and 3mH_{Sar}, CH_3), 2.06–1.21 (br, 6lH_{Lys}, C$_a$H-CH_2-CH_2-CH_2), 2.00 (d, 3H_{Ac}, CH_3), 0.86–0.80 (d, 9H_{Neo}, C(CH_3)$_3$).

2.5. ABC miktoarm star Polymers: (Neo)pSar$_{56}$-Lys(pGlu(OBn)$_{15}$)-pLys(TFA)$_{16}$(Ac)

The synthetic procedure was identical to the previous described AA'B-type miktoarm star polmyers besides the use of respective NCAs and equivalents for the different arms. Starting from (Neo)pSar$_{52}$-Lys-H as macroinitiator, 15 eq of Lys(TFA)-NCA were used for polymerization of the second arm and later 15 eq of Glu(OBn)-NCA were used for polymerization of the third arm. ^{1}H NMR (500 MHz, DMSO-d_6) δ [ppm] = 9.37–9.27 (m, 1mH_{Lys}, N$_\varepsilon$H), 8.25–7.84 (br, 1mH_{Lys}, N$_\alpha$H) and (1lH_{Glu}, N$_\alpha$H), 7.32–7.18(m, 5lH_{Glu}, C$H^{2\text{-}6,Bn}$), 5.09–4.94 (m, 5lH_{Glu}, O-CH_2-Bn), 4.40–3.79 (m, 2nH_{Sar}, CH_2) and (1mH_{Lys}, C$_\alpha$H) and (1lH_{Glu}, C$_\alpha$H), 3.16–3.07 (br, 2mH_{Lys}, N$_\varepsilon$H-CH_2), 2.96–2.73 (m, 3nH_{Sar}, CH_3), 2.39–2.29 (br, 2lH_{Glu}, CH_2-COO), 1.99–1.19 (br, 2lH_{Glu}, C$_\alpha$H-CH_2) and ((N6mH_{Lys}, C$_a$H-CH_2-CH_2-CH_2) and (3H_{Ac}, CH_3), 0.86–0.80 (d, 9H_{Neo}, C(CH_3)$_3$).

3. Results and discussion

It is well established that polypeptoids, such as pSar, can be synthesized by amine-initiated ROP under living conditions.[54–57] Consequently, reactive polymer end groups allow for quantitative functionalization by post-polymerization modifications which has already been demonstrated for e.g. chain end quenching by acetylation, azide-introduction or dye-conjugation by active-ester chemistry. [31,58–60] Within this study we use neopentylamine (Neo) as initiator for the ROP of Sar-NCA, as the *tert*-butyl end group allows for good ^{1}H NMR characterizability, and functionalize the resulting pSar with Fmoc-Lys(Boc)-OPfp by reactive-ester chemistry. As shown in Scheme 1, the introduction of this multifunctional end groups, containing the orthogonal protective groups Fmoc and Boc, allows for sequential deprotection of the Lys amines, starting from Fmoc as will be discussed later, followed by polymerization of the respective arm again by amine-initiated ROP of NCAs. To prevent interference of the second arm's active chain end with the third arm's polymerization, we performed an acetylation (Ac) for inactivation.

With focus to access the gap between linear AB diblock and A_3B polypept(o)ide star polymers [51] and to create the foundation for a siRNA delivery system based on charge-matching Y-shaped polymers [61] allowing to modulate the density of stealth-like polymers at the polyion core polymer corona interphase, we utilized this approach for the synthesis of AA'B PeptoMiktoStars, where B is targeted to be a pLys segment with chain length of ~ 20. As both pSar arms (A) are synthesized separately and not in parallel, they are considered to be not identical and therefore described as AA' instead of A_2. To present the utility of this approach for different star polymers, we performed the synthesis of small and big pSar-macroinitiators with chain lengths of X_n 50 or 150, respectively. To verify the controlled and facile synthesis, ^{1}H NMR, including ^{1}H DOSY experiments, and *SEC* (in HFIP) have been conducted in parallel. As shown in Fig. 1**A**, all proton species of the functionalized macroinitiator (Neo)pSar-Lys(Boc)-Fmoc can be assigned to the ^{1}H NMR spectrum. Integration of the distinct Neo end group (0.82–0.86 ppm) was utilized for determination of the pSar chain length by comparison to respective integrals of the repeating units (4.38–3,93 ppm and 3.00–2.73 ppm) and determined as X_n = 56 for the small macroinitiator. With the limits of NMR analytics, integrals of Fmoc (7.88 ppm, 7.73 ppm, 7.41 ppm and 7.32 ppm) and Boc (1.36 ppm) signals indicate quantitative end group conversion. Assigning proton signals to different diffusing species, ^{1}H DOSY NMR verified structural integrity, presenting initiator, Fmoc and Boc signals at the same polymeric diffusing species of pSar with absence of any detectable Fmoc-Lys(Boc)-OPfp impurities that could hamper ^{1}H NMR interpretation as well as impairing the control of the following polymerization steps. In order to utilize this structure as macroinitiator for polymerization of the second arm, Fmoc protective group was removed as verified by disappearance of the related signals at 7.88–7.32 ppm within the ^{1}H NMR

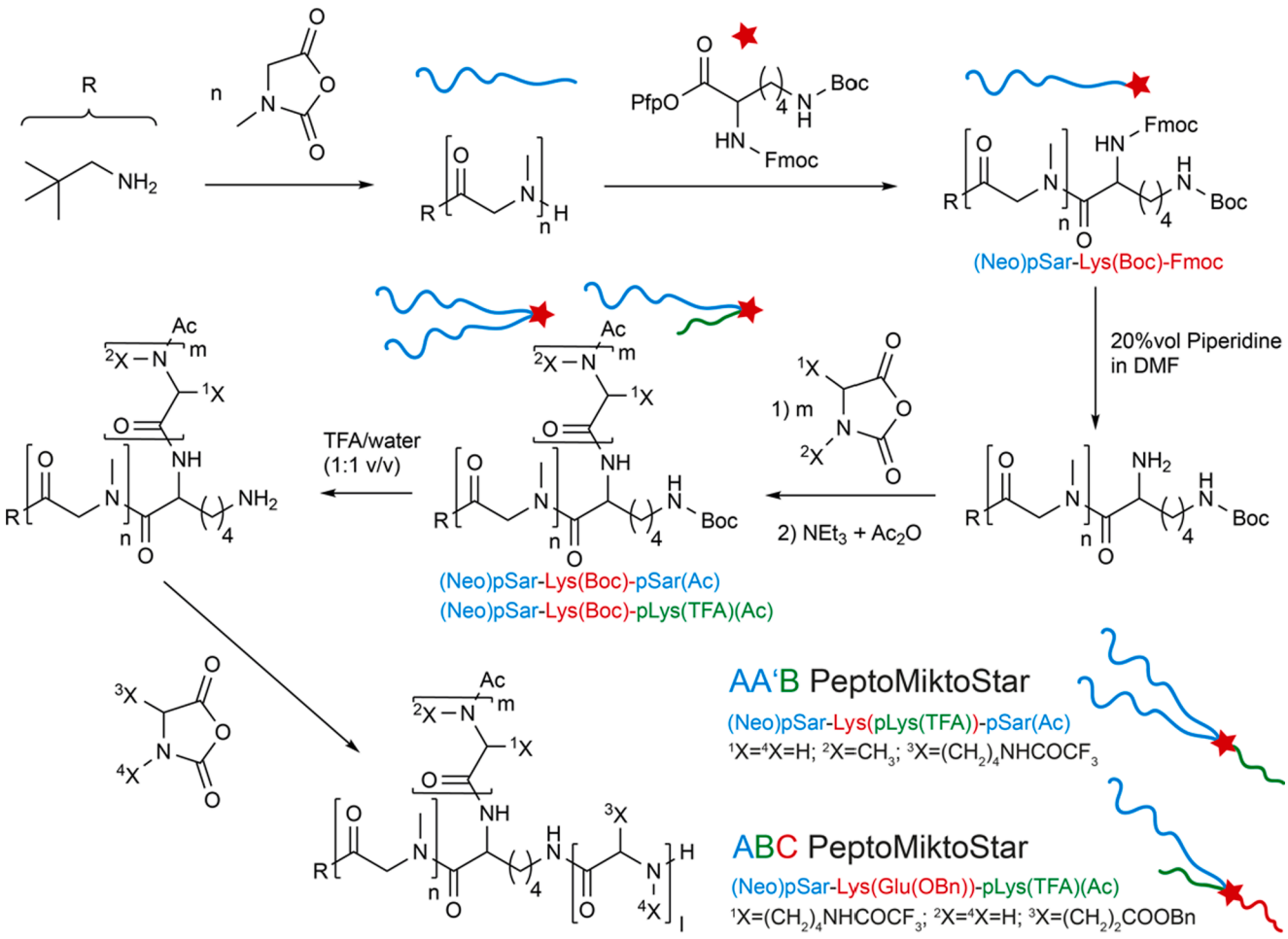

Scheme 1. Cross-over synthetic route for AA'B and ABC PeptoMiktoStars based on Lys(Boc)-Fmoc-functionalization of a pSar polymer.

(Fig. 1**C**) as well as the ^{1}H DOSY spectrum (**Fig. S1**). Similar analytical results are obtained for the second macroinitiator with a determined chain length of $X_n = 156$ (**Fig. S2**). *SEC* experiments further revealed controlled synthesis, demonstrating monomodal elugrams with Poisson-like and narrow molecular weight distribution ($Đ \leq 1.11$) in all cases (Fig. 1**D**).

Resistance of the polymeric backbone against Fmoc-deprotection conditions is further revealed by *SEC*. While no changes in *SEC* elugrams can be observed for the bigger macroinitiator, minor elugram alterations in the smaller one derive from end group effects (polarity, hydrogen bonds) of the terminal amine upon Fmoc-removal. Additional validation of the determined chain lengths was obtained by comparison of the elution maxima to a pSar calibration[26], giving $X_n = 61$ and 155 for the (Neo)pSar-Lys(Boc)-Fmoc species, respectively. However, with respect to the influence of the Lys(Boc)-Fmoc end group, ^{1}H NMR analytics are considered to be more accurate. Synthetically, it is worth mentioning that dialysis as work up of the latter step was necessary to remove residual piperidine impurities. Even below the ^{1}H NMR detection limit, we experienced appearance of a second polymeric species upon the polymerization of the second arm without prior dialysis, most likely due to co-initiation by piperidine traces. Importantly, the sequence of protective group removal steps played a major role, as control over the second arm polymerization could only be guaranteed when Fmoc removal was performed first. Otherwise, the Fmoc group was suspected to present insufficient stability against the liberated amine of the Lys side chain and consequently to interfere with the following NCA polymerization steps.

In order to firstly synthesize symmetrical AA' precursors for the synthesis of AA'B PeptoMiktoStars, the previous described (Neo)pSar-Lys(Boc)-H polymers ($X_n = 56$ and 156) were utilized as macroinitiators for synthesis of the second arm, again by ROP of Sar-NCA, followed by acetylation of the chain end. As revealed by *SEC*, constant chain growth was observed by a clear shift of the elugrams while maintenance of monomodal and narrow molecular weight distributions ($Đ < 1.05$) (Fig. 2**A**). Chain lengths of A' were again determined by ^{1}H NMR analysis, calculated by the growth of pSar related integrals ($X_{n,A'} = 53$) and structural integrity demonstrated by ^{1}H DOSY experiments (**Fig. S3**). Moreover, these spectra confirmed the increase of pSar signals in comparison to the Neo initiator signal and the acetylation (2.00 ppm). Upon treatment with TFA/water (1:1 v/v) and subsequent dialysis, removal of the Boc protective group (1.36 ppm) of the pSar-pSar-linking Lys was confirmed by ^{1}H NMR (Fig. 2**C**) and structural integrity as well as resistance against reaction conditions by ^{1}H DOSY (**Fig. S4**) and *SEC* experiments (Fig. 2**A and B**). Taken together, the synthetic procedure can nicely be tracked by comparing the different ^{1}H NMR spectra (Fig. 2**C**). Starting from (Neo)pSar_{56}-Lys(Boc)-Fmoc with constant intensity of the Neo initiator signal, first the Fmoc removal can be observed, then increase of pSar as well as the appearance of acetyl chain end related integrals becomes evident. Supported by *SEC* and ^{1}H DOSY analytics the synthesis of an AA' macroinitiator (Neo)pSar_{56}-Lys-pSar_{53}(Ac) can be verified. Presenting comparable analytical results, summarized in Fig. 2**B and S5**, the greater macroinitiator could be converted into a (Neo)pSar_{156}-Lys-pSar_{123}(Ac) AA' architecture to utilize for the big star variant.

To demonstrate the versatility of this approach and the high control over every single polymerization step, we further synthesized

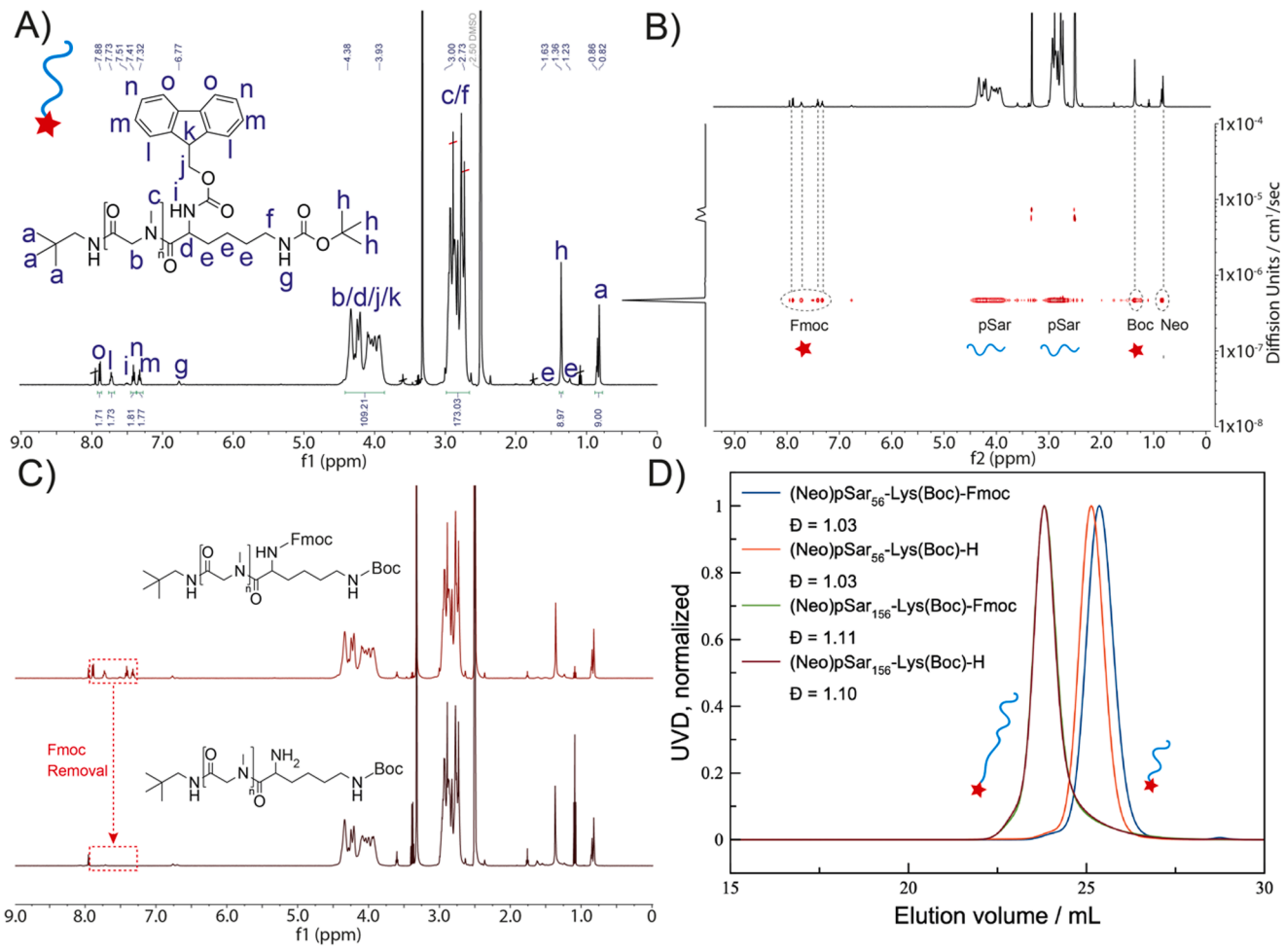

Fig. 1. Characterization of A macroinitiators by A) ^{1}H NMR analysis of (Neo)pSar$_{56}$-Lys(Boc)-Fmoc including B) ^{1}H DOSY NMR spectrum and comparison to C) ^{1}H NMR spectrum after Fmoc-deprotection (500 MHz, DMSO-d_6). D) *SEC* (in HFIP) elugrams of (Neo)pSar$_{56}$-Lys(Boc)-Fmoc and (Neo)pSar$_{156}$-Lys(Boc)-Fmoc before and after Fmoc-deprotection.

asymmetric AA' macroinitiators, comprising one small and one big pSar arm, starting from both directions. In line with previous analytical results, complete ^{1}H NMR, including ^{1}H DOSY, analyses are displayed in **Figs. S6 and S7** and confirmed the controlled synthesis of (Neo)pSar$_{167}$-Lys(Boc)-pSar$_{68}$(Ac) and (Neo)pSar$_{55}$-Lys(Boc)-pSar$_{134}$(Ac) (later used for the asymmetric PeptoMiktoStar). As visualized by the *SEC* elugrams (Fig. 3**A and B**), different sizes of the A macroinitiators can be observed by a lower elution volume of the $X_n = 167$ variant. However, the final AA' architectures showed comparable elution volumes, defined by their comparable final structure, although obtained by two different synthetic routes (**Fig. S8**). Overall, all polymeric structures demonstrated Poisson-like and narrow molecular weight distribution (Đ<1.08), representing controlled synthesis without an indication of side reactions. In summary, the previous described synthetic approach was utilized for the synthesis of different variants of AA' macroinitiators (small, asymmetric and big), which can now serve as initiators for third arm's synthesis by ROP of Lys(TFA)-NCA aiming for $X_{n,Lys} = 20$.

Upon polymerization of the third block, shifts towards lower elution volumes in *SEC* elugrams were observed in comparison to the AA' architectures, confirming increased molecular weights and successful chain extension (exemplary shown for asymmetric PeptoMiktoStar in Fig. 4**A**). Additionally, no small molecular weight species were detected at higher elution volumes, excluding impurity-initiated or single arm polymerizations. Further, molecular weight distributions were kept at low dispersity levels (Đ<1.14), indicating controlled synthesis (**Fig. S9A and B**), although the co-existence of pLys(TFA) in different secondary structures[62] induces in all cases a slight low molecular weight tailing. Successful addition of the third arm under controlled polymerization conditions is supported by ^{1}H NMR analysis, demonstrating the appearance of all pLys(TFA) related proton species (Fig. 4**B**). Distinct signals of the pLys(TFA) side chain's amide proton (9.39–9.25 ppm) and the proximate CH_2-group (3.16.-3.11 ppm) were utilized to calculate pLys(TFA) chain length to be 19 (for small PeptoMiktoStar). ^{1}H DOSY NMR analysis finally verified structural integrity and therefore synthesis of AA'B PeptoMiktoStars by assigning all proton species to a single diffusing species (**Fig. S10A**). Same quality NMR analytics of the asymmetric (**Figs. S10B and C**) and big (**Fig. S10D and E**) PeptoMiktoStars confirmed their synthesis. In line with former publications on pSar-*block*-pLys(TFA) copolymers secondary structure related effects cannot be detected in DMSO. According to the demonstrated results, we were able to verify controlled synthesis of (Neo)pSar$_{56}$-Lys(Lys(TFA)$_{19}$)-pSar$_{53}$(Ac), (Neo)pSar$_{55}$-Lys(Lys(TFA)$_{21}$)-pSar$_{134}$(Ac) and (Neo)pSar$_{156}$-Lys(Lys(TFA)$_{24}$)-pSar$_{123}$(Ac) AA'B architectures by a crossover procedure, introducing the miktoarm's core by end group functionalization of the first pSar arm, summarized in Table 1**,** including precursor polymers. Deviations between theoretical and *SEC*-determined molecular weights derive from the PMMA-*SEC*-calibration and should only be interpretated as trends.

With the feature of control over each arm also in terms of chemical nature, we aimed to further synthesize an ABC-type PeptoMiktoStar. Thus, we utilized a small (Neo)pSar$_{52}$-Lys(Boc)-Fmoc (Đ = 1.03) macroinitiator to initiate ROP of Lys(TFA)-NCA for the second and of Glu

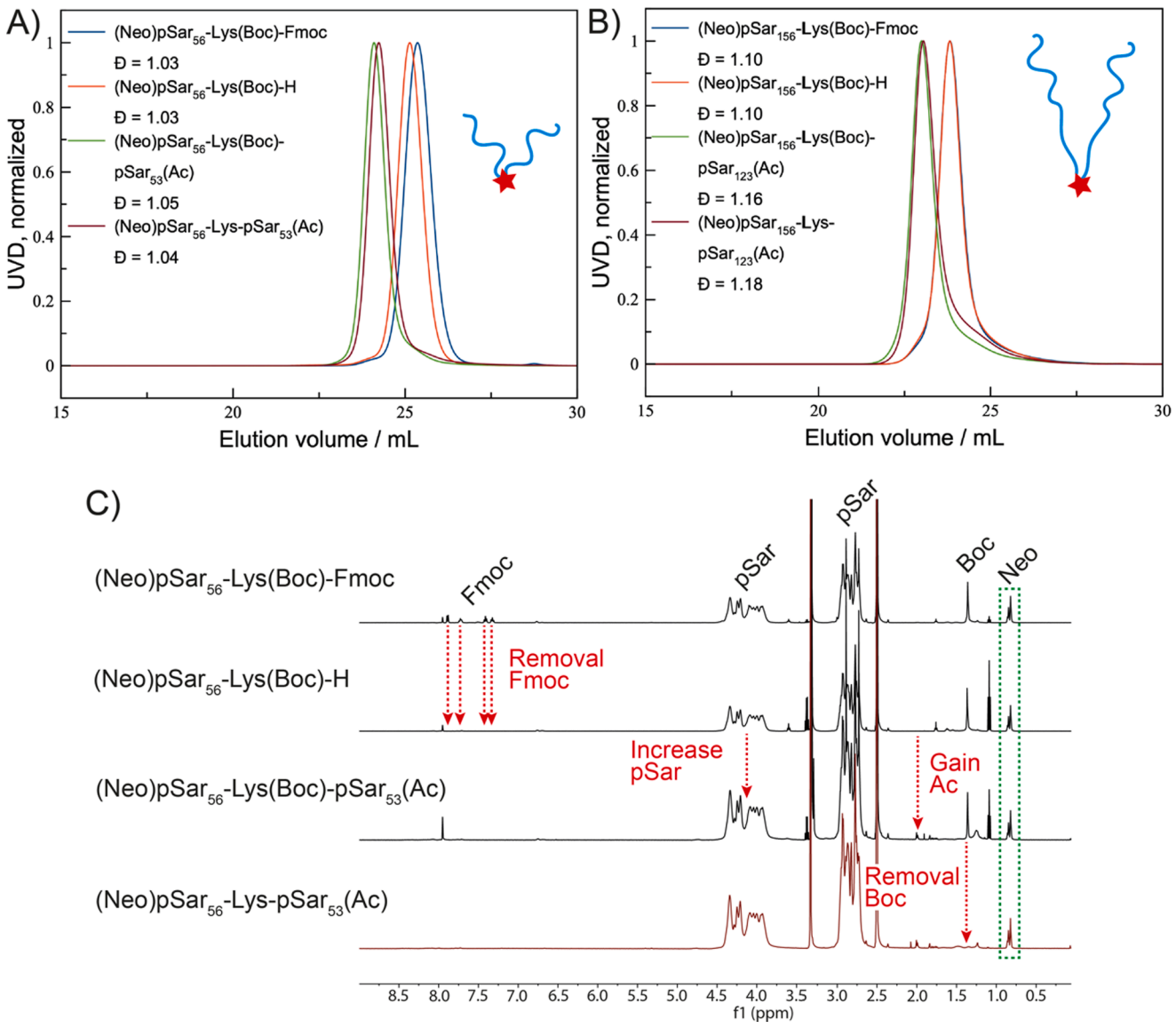

Fig. 2. *SEC* (in HFIP) elugrams of AA' macroinitiators A) (Neo)pSar$_{56}$-Lys(Boc)-pSar$_{53}$(Ac) and B) (Neo)pSar$_{156}$-Lys(Boc)-pSar$_{123}$(Ac), before and after Boc-deprotection and in comparison to their precursors. C) Development of ^{1}H NMR spectra (500 MHz, DMSO-d_6) up to AA' macroinitiator (Neo)pSar$_{56}$-Lys-pSar$_{53}$(Ac) and indicated changes (red) with constant Neoinitiator signal (green). (For interpretation of the references to colour in this figure legend, the reader is referred to the web version of this article.)

(OBn)-NCA for the third arm, each targeted to have chains of 15 repeating units. *SEC* evaluation of the different stages (Fig. 5**A**) revealed an unexpected elugram of the AB architecture as the main peak did not shift to lower but even slightly to higher elution volumes and additionally presenting a dominant fronting. However, as this effect vanished upon third block addition, was not present in ^{1}H DOSY NMR analytics and faultless analytics were obtained for the ABC-structure, we assumed secondary-structure formation to be responsible for it, as already shown for pLys(TFA) polymers.[62] MALDI-TOF MS analysis was not possible for these ABC miktoarm star polymers. The *SEC* elugram of the ABC PeptoMiktoStar reveals a monomodal and narrow molecular weight distributed structure (Đ = 1.10). Moreover, the single block additions were monitored by ^{1}H NMR (Fig. 5**B**), clearly presenting the loss of protective group related proton species as well as the gain of arm B- and C-related proton species within respective synthetical steps. In addition, maintenance of precursor signals in all stages indicated structural integrity through the full synthetic procedure. Utilizing ^{1}H NMR analytics and integration of the distinct Neo initiator signal, chain lengths were determined as previously described and by distinct signals of the benzyl protective group at 7.32–7.18 ppm (5x CH) and 5.09–4.94 ppm (CH_2) for pGlu(OBn) (**Fig. S11**). Thus, the polymeric structure was defined as (Neo)pSar$_{52}$-Lys(pGlu(OBn)$_{15}$)-Lys(TFA)$_{16}$(Ac), in line with the desired chain lengths, further underlining the controlled polymerization. Finally, in ^{1}H DOSY NMR spectrum, all proton species were assigned to a single diffusing species, confirming all three arms sharing one polymeric structure (Fig. 5**C**). Consequently, the successful synthesis of the ABC-PeptoMiktoStar has been described, summarized in Table 1.

4. Conclusion

To conclude, we demonstrated a novel synthetic approach for the versatile design of AA'B- and ABC-type PeptoMiktoStars by introducing a Lys(Boc)-Fmoc end group with active ester chemistry to a pSar chain end. Thus, the orthogonal protective groups enable sequential removal and subsequent amine-initiated controlled living ROP of respective NCAs to form miktoarm architectures, completely based on amino acid repeating units. Separate synthesis of each arm allowed for control over chemical nature and chain lengths and offered a wide range of design

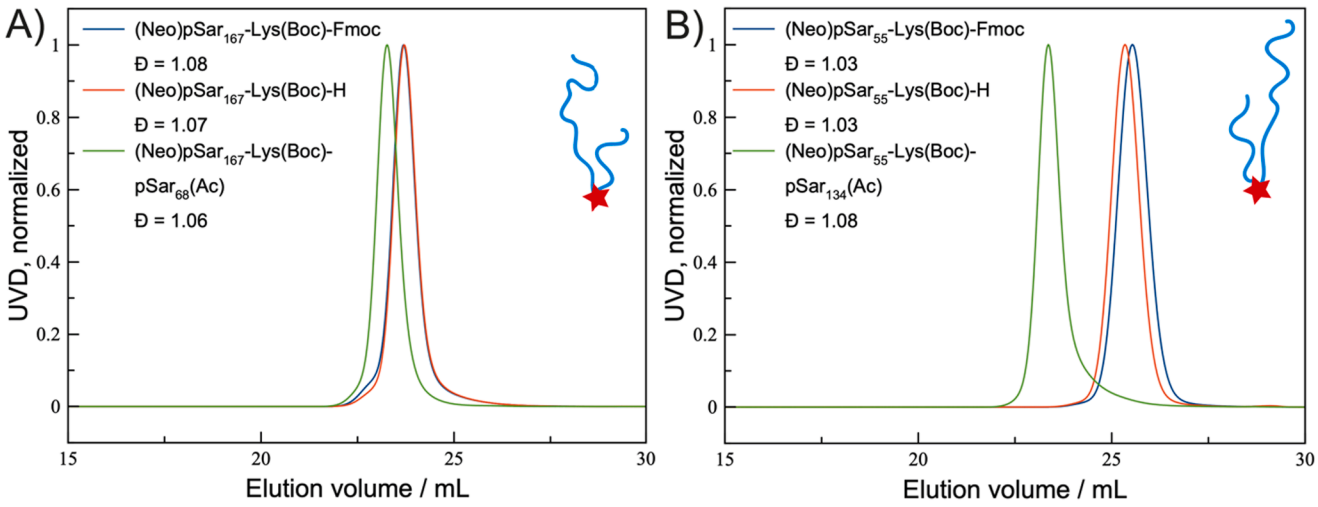

Fig. 3. *SEC* (in HFIP) elugrams of asymmetric AA' macroinitiators A) (Neo)pSar$_{167}$-Lys(Boc)-pSar$_{68}$(Ac) and B) (Neo)pSar$_{55}$-Lys(Boc)-pSar$_{134}$(Ac) in comparison to their precursors.

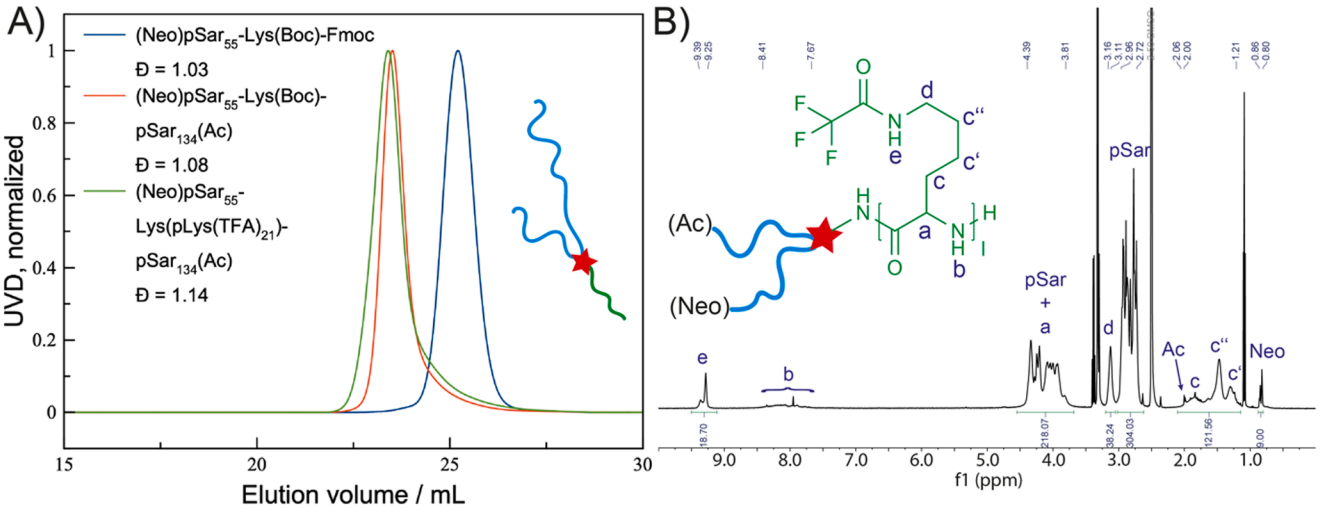

Fig. 4. A) *SEC* (in HFIP) elugrams of AA'B PeptoMiktoStar (Neo)pSar$_{55}$-Lys(pLys(TFA)$_{21}$)-pSar$_{134}$(Ac) in comparison to precursors and B) ^{1}H NMR analysis of (Neo)pSar$_{56}$-Lys(pLys(TFA)$_{19}$)-pSar$_{53}$(Ac) (500 MHz, DMSO-d_6).

Table 1
Summary of analytical results of synthesized PeptoMiktoStars including precursor polymers.

Architecture	Stage[a]	X_n[b] (calc)	$X_{n,A}$[c]	$X_{n,A'/B}$[c]	$X_{n,B/C}$[c]	M_n[d] [g·mol^{-1}]	Đ[d]
AA'B (small)	A	50	56			15,700	1.03
	AA'	50	56	53		26,700	1.05
	AA'B	20	**56**	**53**	**19**	**31,500**	**1.11**
AA'B (asym.)	A	50	55			14,600	1.03
	AA'	150	55	134		34,100	1.08
	AA'B	20	**55**	**134**	**21**	**35,600**	**1.12**
AA'B (big)	A	150	156			27,500	1.11
	AA'	150	156	123		38,900	1.16
	AA'B	20	**156**	**123**	**24**	**40,200**	**1.14**
ABC	A	50	52			14,100	1.03
	AB	15	52	16		17,000	1.09
	ABC	15	**52**	**16**	**15**	**24,400**	**1.10**

[a] respective variants before protective group removal (Fmoc or Boc).
[b] aimed chain length for the upcoming arm, adjusted by ratio of initiator to monomer.
[c] calculated by ^{1}H NMR spectra (in DMSO).
[d] calculated by *SEC* (in HFIP), related to PMMA-calibration.

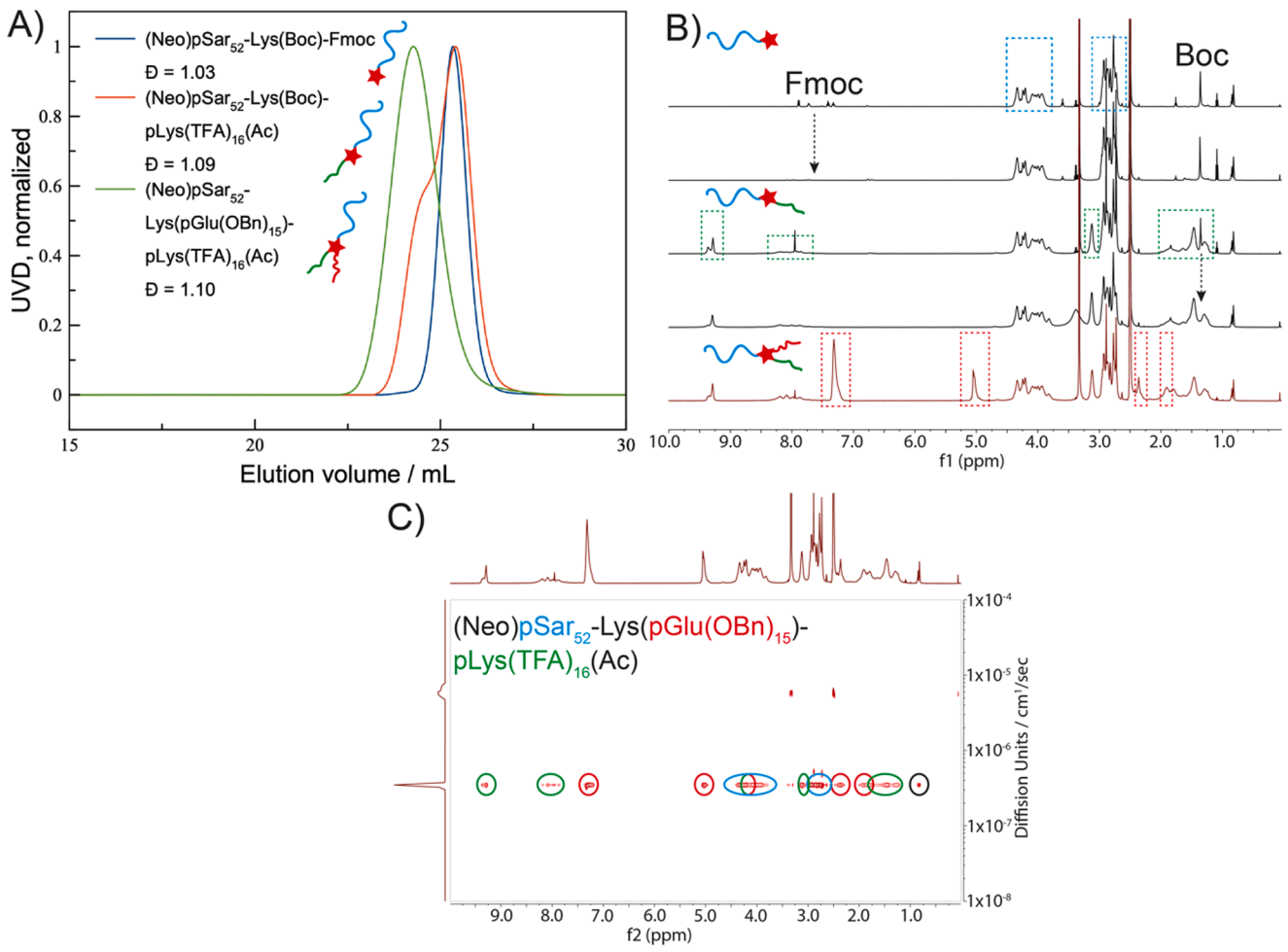

Fig. 5. A) *SEC* (in HFIP) elugram of ABC PeptoMiktoStar (Neo)pSar$_{52}$-Lys(pGlu(OBn)$_{15}$)-pLys(TFA)$_{16}$(Ac) in comparison to precursors. B) Development of ^{1}H NMR spectra (500 MHz, DMSO-d_6) with constant neopentylamine initiator signal. Respective pSar signals are marked in blue, pLys(TFA) signals in green, pGlu(OBn) signals in red and changes upon protective group removals with black arrows. C) ^{1}H DOSY NMR of (Neo)pSar$_{52}$-Lys(pGlu(OBn)$_{15}$)-pLys(TFA)$_{16}$(Ac) (500 MHz, DMSO-d_6). (For interpretation of the references to colour in this figure legend, the reader is referred to the web version of this article.)

opportunities. We presented the synthesis of a small, asymmetric and big AA'B PeptoMiktoStar with narrow molecular weight distributions, comprising two pSar arms of $X_n \sim 50$ and ~ 150 in different combinations paired with a pLys(TFA) arm of $X_n \sim 20$. ^{1}H NMR analytics enabled detailed monitoring of the synthetic procedure, *SEC* and ^{1}H DOSY NMR moreover confirmed star architectures. The high versatility of this approach was further utilized to design an ABC PeptoMiktoStar based on pSar, pLys(TFA) and pGlu(OBn). Therefore, we extended the current library of polypept(o)ide-based star architectures and filled the gap between linear polypept(o)ides and A_3B PeptoMiktoStars. The described polymeric architectures and also the approach itself will lead to novel nanocarrier systems for drug and gene delivery.

Funding

We would like to acknowledge financial support by the German Research Foundation (DFG) within the Collaborative Research Centre SFB1066-3 Project B12 and B5.

CRediT authorship contribution statement

Leon Capelôa: Conceptualization, Methodology, Validation, Investigation, Data curation, Writing – original draft, Visualization, Project administration. **David Schwiertz:** Writing – review & editing, Visualization. **Matthias Barz:** Conceptualization, Resources, Writing – review & editing, Supervision, Project administration.

Declaration of Competing Interest

The authors declare the following financial interests/personal relationships which may be considered as potential competing interests: Matthias Barz reports a relationship with Curapath that includes: board membership and consulting or advisory.

Data availability

Data will be made available on request.

Appendix A. Supplementary data

Supplementary data to this article can be found online at https://doi.org/10.1016/j.eurpolymj.2023.111896.

References

[1] J.W. Mays, Polym. Bull. 23 (1990) 247.
[2] H. Iatrou, N. Hadjichristidis, Macromolecules 25 (1992) 4649.
[3] N. Hadjichristidis, J. Polym. Sci. Part A Polym. Chem. 37 (1999) 857.
[4] N. Hadjichristidis, H. Iatrou, M. Pitsikalis, J. Mays, Prog. Polym. Sci. 31 (2006) 1068.
[5] V. Lotocki, A. Kakkar, Pharmaceutics 12 (2020) 827.

[6] M. Liu, J.R. Blankenship, A.E. Levi, Q. Fu, Z.M. Hudson, C.M. Bates, Chem. Mater. 34 (2022) 6188.
[7] K. Khanna, S. Varshney, A. Kakkar, Polym. Chem. 1 (2010) 1171.
[8] M. Baghbanbashi, A. Kakkar, Mol. Pharm. 19 (2022) 1687.
[9] P. Salas-Ambrosio, A. Tronnet, M. Badreldin, L. Reyes, M. Since, S. Bourgeade-Delmas, B. Dupuy, P. Verhaeghe, C. Bonduelle, Polym. Chem. 13 (2022) 600.
[10] H. Jin, T. Jian, Y. Ding, Y. Chen, P. Mu, L. Wang, C. Chen, Biopolymers 110 (2019) e23258.
[11] Y. Zhang, H. Liu, J. Hu, C. Li, S. Liu, Macromol. Rapid Commun. 30 (2009) 941.
[12] B. Sui, H. Xu, J. Jin, J. Gou, J. Liu, X. Tang, Y. Zhang, J. Xu, H. Zhang, X. Jin, Molecules 19 (2014) 11915.
[13] P.-F. Gou, W.-P. Zhu, N. Xu, Z.-Q. Shen, J. Polym. Sci. Part A Polym. Chem. 47 (2009) 6962.
[14] H. Yin, S.W. Kang, Y.H. Bae, Macromolecules 42 (2009) 7456.
[15] K. Yoon, H.C. Kang, L. Li, H. Cho, M.K. Park, E. Lee, Y.H. Bae, K.M. Huh, Polym. Chem. 6 (2015) 531.
[16] G. Maglio, F. Nicodemi, C. Conte, R. Palumbo, P. Tirino, E. Panza, A. Ianaro, F. Ungaro, F. Quaglia, Biomacromolecules 12 (2011) 4221.
[17] M. Aghajanzadeh, S. Andalib, H. Danafar, K. Rostamizadeh, A. Sharafi, Int. J. Pharm. 586 (2020), 119546.
[18] Y. Ge, C. Chen, X.M. Sim, J. Zheng, A. Goto, Macromol. Rapid Commun. 41 (2020) 1.
[19] J. Wu, W. Sun, X. He, Eur. Polym. J. 137 (2020), 109930.
[20] F. Nederberg, E. Appel, J.P.K. Tan, H.K. Sung, K. Fukushima, J. Sly, R.D. Miller, R. M. Waymouth, Y.Y. Yang, J.L. Hedrick, Biomacromolecules 10 (2009) 1460.
[21] M. Barz, R. Luxenhofer, R. Zentel, M.J. Vicent, Polym. Chem. 2 (2011) 1900.
[22] K. Son, M. Ueda, K. Taguchi, T. Maruyama, S. Takeoka, Y. Ito, J. Control. Release 322 (2020) 209.
[23] L. Hong, Z. Wang, X. Wei, J. Shi, C. Li, J. Pharmacol. Toxicol. Methods 102 (2020), 106678.
[24] I. Hamad, A.C. Hunter, J. Szebeni, S.M. Moghimi, Mol. Immunol. 46 (2008) 225.
[25] S.S. Nogueira, A. Schlegel, K. Maxeiner, B. Weber, M. Barz, M.A. Schroer, C. E. Blanchet, D.I. Svergun, S. Ramishetti, D. Peer, P. Langguth, U. Sahin, H. Haas, A. C.S. Appl, Nano Mater. 3 (2020) 10634.
[26] B. Weber, A. Birke, K. Fischer, M. Schmidt, M. Barz, Macromolecules 51 (2018) 2653.
[27] P.H. Maurer, D. Subrahmanyam, E. Katchalski, E.R. Blout, J. Immunol. 83 (1959) 193.
[28] G.M. Whitesides, B. Grzybowski, Science 295 (2002) 2418.
[29] I. Negwer, A. Best, M. Schinnerer, O. Schäfer, L. Capeloa, M. Wagner, M. Schmidt, V. Mailänder, M. Helm, M. Barz, H.-J. Butt, K. Koynov, Nat. Commun. 9 (2018) 5306.
[30] I. Alberg, S. Kramer, M. Schinnerer, Q. Hu, C. Seidl, C. Leps, N. Drude, D. Möckel, C. Rijcken, T. Lammers, M. Diken, M. Maskos, S. Morsbach, K. Landfester, S. Tenzer, M. Barz, R. Zentel, Small 16 (2020) 1907574.
[31] S. Bleher, J. Buck, C. Muhl, S. Sieber, S. Barnert, D. Witzigmann, J. Huwyler, M. Barz, R. Süss, Small 15 (2019) 1904716.
[32] P. Heller, D. Hobernik, U. Lächelt, M. Schinnerer, B. Weber, M. Schmidt, E. Wagner, M. Bros, M. Barz, J. Control. Release 258 (2017) 146.
[33] L. Capelôa, M. Yazdi, H. Zhang, X. Chen, Y. Nie, E. Wagner, U. Lächelt, M. Barz, Macromol. Rapid Commun. 43 (2022) 2100698.
[34] K. Johann, T. Bohn, F. Shahneh, N. Luther, A. Birke, H. Jaurich, M. Helm, M. Klein, V.K. Raker, T. Bopp, M. Barz, C. Becker, Nat. Commun. 12 (2021) 1.
[35] T.A. Bauer, N.K. Horvat, O. Marques, S. Chocarro, C. Mertens, S. Colucci, S. Schmitt, L.M. Carrella, S. Morsbach, K. Koynov, F. Fenaroli, P. Blümler, M. Jung, R. Sotillo, M.W. Hentze, M.U. Muckenthaler, M. Barz, Adv. Healthc. Mater. 10 (2021) 2100385.
[36] D. Skoulas, V. Stuettgen, R. Gaul, S.-A. Cryan, D.J. Brayden, A. Heise, Biomacromolecules 21 (2020) 2455.
[37] D. Skoulas, S. Fattah, D. Wang, S. Cryan, A. Heise, Macromol. Biosci. 22 (2022) 2200175.
[38] R. Holm, D. Schwiertz, B. Weber, J. Schultze, J. Kuhn, K. Koynov, U. Lächelt, M. Barz, Macromol. Biosci. 20 (2020) 1900152.
[39] M. Darguzyte, R. Holm, J. Baier, N. Drude, J. Schultze, K. Koynov, D. Schwiertz, S. M. Dadfar, T. Lammers, M. Barz, F. Kiessling, Bioconjug. Chem. 31 (2020) 2691.
[40] C. Kappel, C. Seidl, C. Medina-Montano, M. Schinnerer, I. Alberg, C. Leps, J. Sohl, A.K. Hartmann, M. Fichter, M. Kuske, J. Schunke, G. Kuhn, I. Tubbe, D. Paßlick, D. Hobernik, R. Bent, K. Haas, E. Montermann, K. Walzer, M. Diken, M. Schmidt, R. Zentel, L. Nuhn, H. Schild, S. Tenzer, V. Mailänder, M. Barz, M. Bros, S. Grabbe, ACS Nano 15 (2021) 15191.
[41] E.J.L. Stéen, J.T. Jørgensen, K. Johann, K. Nørregaard, B. Sohr, D. Svatunek, A. Birke, V. Shalgunov, P.E. Edem, R. Rossin, C. Seidl, F. Schmid, M.S. Robillard, J. L. Kristensen, H. Mikula, M. Barz, A. Kjær, M.M. Herth, ACS Nano 14 (2020) 568.
[42] K. Klinker, M. Barz, Macromol. Rapid Commun. 36 (2015) 1943.
[43] A. Birke, D. Huesmann, A. Kelsch, M. Weilbächer, J. Xie, M. Bros, T. Bopp, C. Becker, K. Landfester, M. Barz, Biomacromolecules 15 (2014) 548.
[44] W. Vayaboury, O. Giani, H. Cottet, A. Deratani, F. Schué, Macromol. Rapid Commun. 25 (2004) 1221.
[45] T. Aliferis, H. Iatrou, N. Hadjichristidis, Biomacromolecules 5 (2004) 1653.
[46] G.J.M. Habraken, M. Peeters, C.H.J.T. Dietz, C.E. Koning, A. Heise, Polym. Chem. 1 (2010) 514.
[47] H.R. Kricheldorf, α-Aminoacid-N-Carboxy-Anhydrides and Related Heterocycles, Springer-Verlag, Berlin Heidelberg, 1987.
[48] R. Holm, M. Douverne, B. Weber, T. Bauer, A. Best, P. Ahlers, K. Koynov, P. Besenius, M. Barz, Biomacromolecules 20 (2019) 375.
[49] R. Holm, B. Weber, P. Heller, K. Klinker, D. Westmeier, D. Docter, R.H. Stauber, M. Barz, Macromol. Biosci. 17 (2017) 1600514.
[50] R.M. England, J.I. Moss, A. Gunnarsson, J.S. Parker, M.B. Ashford, Biomacromolecules 21 (2020) 3332.
[51] D. Schwiertz, R. Holm, M. Barz, Polym. J. 52 (2020) 119.
[52] H.E. Gottlieb, V. Kotlyar, A. Nudelman, J. Org. Chem. 62 (1997) 7512.
[53] P. Heller, A. Birke, D. Huesmann, B. Weber, K. Fischer, A. Reske-Kunz, M. Bros, M. Barz, Macromol. Biosci. 14 (2014) 1380.
[54] R. Luxenhofer, C. Fetsch, A. Grossmann, J. Polym. Sci. Part A Polym. Chem. 51 (2013) 2731.
[55] J. Ulbricht, R. Jordan, R. Luxenhofer, Biomaterials 35 (2014) 4848.
[56] C. Fetsch, A. Grossmann, L. Holz, J.F. Nawroth, R. Luxenhofer, Macromolecules 44 (2011) 6746.
[57] P. Salas-Ambrosio, A. Tronnet, M. Badreldin, S. Ji, S. Lecommandoux, S. Harrisson, P. Verhaeghe, C. Bonduelle, Polym. Chem. 13 (2022) 6149.
[58] O. Schäfer, K. Klinker, L. Braun, D. Huesmann, J. Schultze, K. Koynov, M. Barz, ACS Macro Lett. 6 (2017) 1140.
[59] B. Weber, C. Seidl, D. Schwiertz, M. Scherer, S. Bleher, R. Süss, M. Barz, Polymers 8 (2016) 427.
[60] K. Klinker, R. Holm, P. Heller, M. Barz, Polym. Chem. 6 (2015) 4612.
[61] S. Watanabe, K. Hayashi, K. Toh, H.J. Kim, X. Liu, H. Chaya, S. Fukushima, K. Katsushima, Y. Kondo, S. Uchida, S. Ogura, T. Nomoto, H. Takemoto, H. Cabral, H. Kinoh, H.Y. Tanaka, M.R. Kano, Y. Matsumoto, H. Fukuhara, S. Uchida, M. Nangaku, K. Osada, N. Nishiyama, K. Miyata, K. Kataoka, Nat. Commun. 10 (2019) 1894.
[62] D. Huesmann, A. Birke, K. Klinker, S. Türk, H.J. Räder, M. Barz, Macromolecules 47 (2014) 928.